

Bipartite Interference and Air Pollution Transport: Estimating Health Effects of Power Plant Interventions

Corwin Zigler¹, Laura Forastiere², and Fabrizia Mealli³

¹ *University of Texas at Austin*

² *Yale University*

³ *University of Florence*

Abstract

Evaluating air quality interventions is confronted with the challenge of interference since interventions at a particular pollution source likely impact air quality and health at distant locations and air quality and health at any given location are likely impacted by interventions at many sources. The structure of interference in this context is dictated by complex atmospheric processes governing how pollution emitted from a particular source is transformed and transported across space, and can be cast with a bipartite structure reflecting the two distinct types of units: 1) *interventional units* on which treatments are applied or withheld to change pollution emissions; and 2) *outcome units* on which outcomes of primary interest are measured. We propose new estimands for bipartite causal inference with interference that construe two components of treatment: a “key-associated” (or “individual”) treatment and an “upwind” (or “neighborhood”) treatment. Estimation is carried out using a semi-parametric adjustment approach based on joint propensity scores. A reduced-complexity atmospheric model is deployed to characterize the structure of the interference network by modeling the movement of air parcels through time and space. The new methods are deployed to evaluate the effectiveness of installing flue-gas desulfurization scrubbers on 472 coal-burning power plants (the interventional units) in reducing Medicare hospitalizations among 22,603,597 Medicare beneficiaries residing across 23,675 ZIP codes in the United States (the outcome units).

Keywords: Causal inference; Potential outcomes; Network interference; Unconfoundedness; Generalized propensity scores; Subclassification.

1 Introduction

Evaluating public-health interventions is increasingly challenged by inherent interconnect-edness of observational units, often cast as a network with observational units as nodes and connections between them as edges. Causal inference in such settings is often confronted with *interference*, which arises when outcomes for some units depend in part on treatments applied to other units. The most typical examples include vaccine interventions with effects propagating across infection networks of individuals who come into contact with one another and informational interventions on individuals connected through their social network. Methods for causal inference with interference have motivated much recent work (Hudgens and Halloran, 2008; Bowers et al., 2013; Liu and Hudgens, 2014; Aronow and Samii, 2017; Karwa and Airola, 2018; Tchetgen and VanderWeele, 2012; Liu and Hudgens, 2014; Liu et al., 2016; Forastiere et al., 2018, 2020; Sävje et al., 2017; An, 2018; Papadogeorgou et al., 2019; An and VanderWeele, 2019).

Work in Zigler and Papadogeorgou (2020) introduced the setting of *bipartite causal inference with interference*, where the network of observational units consists of two distinct types: *interventional units*, on which treatments are applied or withheld, and *outcome units* on which outcomes of interest are defined and measured. The present work shares the same motivating setting as in Zigler and Papadogeorgou (2020), where interventions to reduce harmful pollution emissions are employed at power plants (the interventional units) and health outcomes of interest are measured at specific population locations (ZIP codes, the outcome units). Interference in this case arises due to phenomena known as *pollution transport and chemistry*; chemical compounds such as sulfur dioxide (SO_2) emitted from a power plant smokestack are transported through the atmosphere and react chemically with atmospheric co-constituents. The primary end product of atmospheric SO_2 is sulfate (SO_4^{2-}), which condenses quickly and contributes to increased particulate air pollution (PM). Therefore, an intervention employed at one power plant will likely affect health outcomes in the locations where chemical compounds are transported. PM of 2.5 microns or less in size ($\text{PM}_{2.5}$) has been associated with a variety of adverse health outcomes (Pope III et al., 2009; Dominici et al., 2014), and is a frequent downstream target of air pollution regulations. Zigler and Papadogeorgou (2020) offered inverse probability of treatment weighted (IPTW) estimators in the simplified setting of bipartite partial interference, where power plants were clustered geographically into non-overlapping groups. The IPTW estimators hewed closely to existing development for partial interference in observational studies (Perez-Heydrich et al., 2014; Tchetgen and VanderWeele, 2012; Liu and Hudgens, 2014; Liu et al., 2016; Papadogeorgou

et al., 2019). The approximation entailed in the clustering and the partial interference assumption employed in previous work is an obvious limitation in light of the true long-range nature of pollution transport that may not cohere to the structure of geographic clusters. Expansion to settings that more realistically reflect the true nature of interference due to pollution transport are clearly warranted.

To confront the challenge of bipartite causal inference with interference without reliance on the partial interference assumption, we continue development from Forastiere et al. (2020) to estimate bipartite versions of direct and indirect (or spillover) effects. Importantly, this work will not rely on a specified clustering of units, nor will it make use of individual average potential outcomes under specified clustered treatment allocations, as in a large swath of development for interference in observational studies (Hudgens and Halloran, 2008; Perez-Heydrich et al., 2014; Tchetgen and VanderWeele, 2012; Liu and Hudgens, 2014; Liu et al., 2016; Papadogeorgou et al., 2019). Rather, the approach allows interference to take place on a structural network and construes the “treatment” under investigation in two components: a “key associated” treatment characterizing a characteristic of the intervention that is specific to an individual location (e.g., whether the power plant most impacting that location adopts the intervention), and a “neighborhood” or “upwind treatment” characterizing treatments among interfering units (e.g., a function of the treatment statuses of power plants located upwind from a location). Reducing the intervention of interest to these two components helps focus the definition of potential outcomes of interest, so that causal estimands and an assignment mechanism can be formalized in the bipartite setting. Estimation of causal effects is based on a joint propensity score model for the two treatment components. While the specifics of the estimation strategy closely follow those in Forastiere et al. (2020), the bipartite nature of the problem requires development of new relevant estimands and some nontrivial differences in formulation of the assignment mechanism, both of which have important implications for how causal effects can be interpreted in light of common threats to validity inherent to observational studies on networks such as homophily and confounding.

An important feature of this work is the manner in which we characterize the mechanistic phenomena underlying the structure of interference. Unlike the common setting where interference arises due to unit-to-unit outcome dependencies (e.g., one person’s vaccination status impacts another person’s infection risk), interference in this case arises due to complex exposure patterns governed by the movement of air pollution from an originating source (a power plant) across long distances towards impact on populations. Interference due to complex exposure patterns (or treatment diffusion) has been considered in the causal inference literature, albeit with less frequency than settings of interference due to unit-to-unit

outcome dependencies and only emerging focus on explicitly spatial data (Verbitsky-Savitz and Raudenbush, 2012; Graham et al., 2013; An, 2018; An and VanderWeele, 2019; Giffin et al., 2020). To characterize the structure of interference, we deploy a newly-developed reduced-complexity atmospheric model, called HYSPLIT Average Dispersion (HyADS), to model the movement of pollution through space and time (Henneman et al., 2019a). HyADS has been recently used in epidemiological studies of exposure to power plant pollution (Henneman et al., 2019b; Casey et al., 2020), but in a manner that collapses exposure metrics across individual power plants, precluding inferences about interventions applied at individual plants. In contrast, this work uses the HyADS model to characterize the bipartite network of relationships between interventional units and outcome units, leading to a notion of a “neighborhood” or “upwind” treatment. The characterization of a network that is not based on notions of contacts or adjacency necessitates careful attention to the definition of useful estimands in the bipartite setting. The analysis of a bipartite network that is characterized by the combination of geography and atmospheric conditions holds more general relevance for methods to address causal inference and interference with spatially-indexed data generally.

The specific intervention evaluated here is the installation (or not) of flue-gas desulfurization scrubbers (“scrubbers”) on 472 coal-fired power plants in the United States during 2005, a year of significant regulatory action on power plants. Such scrubbers are known to reduce emissions of SO_2 , which is an important precursor to the eventual formation of secondary $\text{PM}_{2.5}$ pollution. We deploy the new methods to estimate network intervention effects of scrubber installation on hospitalization outcomes among 22,603,597 adults aged 65 and older enrolled in Medicare and residing across 23,675 ZIP codes. Combining the atmospheric model for pollution transport with novel methods for bipartite causal inference with interference represents an important advance in the methodology available for evaluating interventions at point sources of air pollution.

In order to outline the nature of the bipartite network and interference, Section 2 gives brief background on power plant regulations and describes the atmospheric model that will govern the structure of interference. Section 3 defines potential outcomes, interference mappings, and causal estimands for the bipartite setting. Section 4 outlines the estimation strategy based on generalized propensity scores, which are deployed in the analysis of power plant and Medicare data in Section 5 before concluding with a discussion.

2 Background and Data for Evaluating Power Plant Interventions

2.1 Title IV of the Clean Air Act Amendments and Scrubbers on Coal-Fired Power Plants

Starting with at least Title IV of the 1990 Amendments to the Clean Air Act, air quality management in the US has striven to reduce SO_2 emissions by ten million tons relative to 1980 levels ([Chestnut and Mills, 2005](#)). One motivation for such regulations is the fact that SO_2 is a known precursor to the atmospheric formation of $\text{PM}_{2.5}$, which itself has been linked to myriad adverse health outcomes ([Pope III et al., 2009](#); [Dominici et al., 2014](#)). Thus, a major focus of such efforts to reduce population pollution exposure is the reduction of SO_2 (and other) emissions from coal-fired electricity generating power plants, the dominant source of SO_2 emissions in the US. Strategies to reduce SO_2 emissions at power plants are varied, but one key technology is the installation of a flue-gas desulfurization scrubber (“scrubber”), which is known to initiate substantial reductions in emissions of SO_2 .

2.2 Pollution Transport and HYSPLIT Average Dispersion

One key feature of the link between SO_2 emissions and population health outcomes is the phenomenon of long-range pollution transport, which governs how SO_2 emissions originating at a specific power plant transport across time and space as SO_2 reacts chemically to form SO_4^{2-} and ultimately increases ambient $\text{PM}_{2.5}$ to which populations are exposed. Such transport can render the ambient pollution (and population health) at a particular location susceptible to changes in emissions from power plants located at great distances. Thus, a central task for investigating the impacts of scrubber installation on population health is characterization of which ZIP codes in the US might be affected by scrubber installation at each of the power plants under study.

We use a recently-developed reduced-complexity atmospheric model, called HYSPLIT Average Dispersion (HyADS) to achieve such characterization ([Henneman et al., 2019a](#)). Briefly, HyADS simulates hundreds of thousands of “emissions events” mimicking the release of air mass from the location of each coal power plant smokestack, following each mass forward in time and tracking its movement trajectory (as governed by Lagrangian trajectory mechanics and historical wind field data). Parcel locations are then linked to geographic

locations (e.g., ZIP codes) to generate a metric of the number of times per day each ZIP code is impacted by air originating at each power plant. For this investigation, linked parcel locations for each day are aggregated throughout the entire year of 2005, representing an annual impact of parcels on a given ZIP code location. Details on the HyADS approach appear in [Henneman et al. \(2019a\)](#), where the approach is shown to have good agreement with state-of-the art chemical transport models for air pollution which cannot generally be employed at the computational scale required for the present investigation. The end result of the HyADS simulation is output of a “source-receptor” matrix with entries characterizing each power plant’s annual influence on each ZIP code. This will form the basis of the network adjacency matrix in Section 3.2. Deriving a network adjacency matrix with information representing a physical/chemical process represents an important point of departure from studies on social networks.

2.3 Supporting Data on Power Plants and Zip Codes

In addition to the historical wind fields data underlying the HyADS simulation described in Section 2.2, data on monthly SO₂ emissions for each coal-fired power plant operating in the US were obtained from the US Environmental Protection Agency (EPA) Air Markets Program Database, along with information about power plant characteristics, including the dates of any scrubber installations. HyADS also uses information on the heights of power plant smokestacks, obtained from the US Energy Information Administration. Medicare health outcomes come from the Center for Medicare and Medicaid Services. These data were processed into annual counts (and rates) of hospitalizations for each US ZIP code, along with supporting data on person-years at risk for hospitalization as well as basic demographic characteristics of Medicare beneficiaries. For this evaluation, we focus on hospitalizations for Ischemic Heart Disease (IHD) which has been specifically linked to ambient PM_{2.5} derived from coal combustion in [Thurston et al. \(2016\)](#) and [Henneman et al. \(2019b\)](#). Demographic information on the general population of each ZIP code was obtained from the US Census (year 2000), and county-level smoking rates come from small-area estimated values anchored to the CDC Behavior Risk Factor Surveillance System ([Dwyer-Lindgren et al., 2014](#)). Weather and climatological characteristics for each ZIP code come from the North American Regional Reanalysis ([Kalnay et al., 1996](#)), and a annual average total mass of PM_{2.5} (for use in a secondary analysis) is obtained from GEOS-Chem chemical transport model predictions on a grid across the US and linked to the ZIP code level ().

3 Notation and Estimands for the Bipartite Setting

3.1 Potential Outcomes On Bipartite Networks

Against the backdrop of the power plant problem and data outlined in Section 2, we offer here the development of potential outcomes in settings of bipartite interference, as detailed in [Zigler and Papadogeorgou \(2020\)](#). Let $j = 1, 2, \dots, J$ index a sample of J observational units, at which a well-defined intervention may or may not occur, with an indicator $S_j = 1$ if the j^{th} unit is “treated” with the intervention and $S_j = 0$ otherwise. Call these observational units *interventional units*. In the motivating power plant example, the interventional units are $J = 472$ coal-fired power plants operating in the US in 2005, and $S_j = 1$ denotes that the j^{th} plant had a scrubber installed for at least half of the year. The vector $\mathbf{S} = (S_1, S_2, \dots, S_J)$ denotes the vector of treatment assignments to the J interventional units, taking on a specific value $\mathbf{s} \in \mathcal{S}(J)$, where $\mathcal{S}(J)$ denotes the space of possible such vectors. Denote covariates measured at the interventional units with \mathbf{X}_j^{int} .

Let $i = 1, 2, \dots, n$ index a second, distinct set of observational units where outcomes of interest are defined and measured. Call these units *outcome units*, and let $Y_i, i = 1, 2, \dots, n$ represent an outcome of interest measured at each. For example, in the power plant investigation, Y_i denotes the number of hospital admissions for ischemic heart disease (IHD) in 2005 among Medicare beneficiaries residing in each of $n = 23,675$ ZIP codes across the US. Denote covariates measured at the outcome units with \mathbf{X}_i^{out} for $i = 1, 2, \dots, n$. Settings with observational units, outcomes, and interventions described as above have been referred to as settings of *bipartite causal inference* ([Zigler and Papadogeorgou, 2020](#)).

Note that, without further restrictions or assumptions on the bipartite structure, there is no clear definition of the intervention for the outcome units. Nonetheless, the general goal will be to estimate causal effects of the intervention, S , on the outcome Y . Formalizing such questions can proceed with potential outcomes in the bipartite setting, following in much the same manner as in settings of one level of observational unit. Let $Y_i(\mathbf{s})$ denote the potential outcome that would be observed at outcome unit i under treatment allocation \mathbf{s} , for example, the number of IHD hospitalizations that would occur at the i^{th} ZIP code under a specific allocation of scrubbers to the J power plants. In full generality, for each unit j the number of potential outcomes $Y_i(\mathbf{S})$ correspond to the number of possible allocations in $\mathcal{S}(J)$, for example, 2^J possible treatment vectors when S_j is binary and each interventional unit is eligible for treatment. The key difference owing to the bipartite setting is that \mathbf{S} is a

vector of length J , not a vector of length n , as would be the case under typical development of potential outcomes with one level of observational unit. Implicit in the above notation is the assumption of consistency or “no multiple versions of treatment,” that is, $Y_i(\mathbf{s}) = Y_i(\mathbf{s}')$ for all i when $\mathbf{s} = \mathbf{s}'$.

3.2 Continuous Interference Mappings for Weighted Directed Networks

Typical formulation of potential outcomes would proceed with the so-called Stable Unit Treatment Value Assumption (SUTVA) clarifying, in part, that there is “no interference” between units in the sense that outcomes for a given unit do not depend on treatments applied at other units. The lack of immediate correspondence between interventional units and outcome units in the bipartite setting precludes an immediate statement of SUTVA. While fully general development would allow the outcome at any outcome unit to depend on the treatments assigned at all interventional units, there may be information to support constraints on the structure of interference. These constraints have been previously specified in settings with one type of observational unit with “interference mappings” (Zigler and Papadogeorgou, 2020), “interference sets” (Liu et al., 2016), or “interference neighborhoods” (Karwa and Aioldi, 2018), and such information is often coded with a graph specifying a specific network structure where the set of units that interfere with an index unit consists of those with a limited path distance from the index node, typically those that are adjacent “neighbors” in the network (Forastiere et al., 2020). In standard settings, the interference set is specified on a one-mode network, representing interconnections between units. In the bipartite setting, where actions at interventional units can impact outcome units, but not *vice versa*, interference mapping should be defined on a different kind of network structure, with two sets of nodes and ties linking nodes belonging to different sets. This structure can be regarded as a *bipartite (or two-mode) directed* network.

Settings where interference arises due to complex exposure patterns invites specification of interference structures that expand beyond discrete notions of interference sets to encode continuous degrees of interference that depend on the propagation or diffusion of exposure across the network. In particular, while interference sets in social networks are typically defined *topologically*, we consider settings where interference is more aptly viewed *geographically* or *physically*, as dictated by a (continuous) underlying process. For example, for interventions applied to spatially-indexed units, the degree of interference between two units may be dictated in part by the geographic distance between them or, in the case of the power

plant study, the geographic distance and features of the atmospheric processes that transport pollution from sources to populations. Thus, in the power plant setting, the structure of interconnectedness between interventional and outcome units can be regarded as a *bipartite weighted and directed* network.

For such a bipartite weighted and directed network, we expand the notion of an *interference mapping* from [Zigler and Papadogeorgou \(2020\)](#). Specifically, let $t_i^\top = (t_{i1}, t_{i2}, \dots, t_{iJ})$ denote outcome-unit specific interference map for the i^{th} outcome unit, with t_{ij} quantifying the weighted connectedness between interventional unit j and the outcomes defined at outcome unit i . The sample interference map can then be defined as $T = (t_1, t_2, \dots, t_n)^\top$, an $N \times J$ matrix with (i,j) entry indicating the strength of influence of the j^{th} interventional unit on the potential outcome for the i^{th} outcome unit. In the power plant evaluation, the entries of T are generated directly from HyADS simulations, representing the aforementioned source-receptor matrix. Note that this characterization of interference in the power plant setting is based only on wind fields and parcel movement trajectories, and is not affected by scrubber installations, that is, T is fixed and not affected by S . Previous epidemiological investigations have not used T directly, but collapsed over the rows of T to define a single metric of total exposure (weighted by emissions) for each outcome unit, and then estimated associations between health outcomes and this metric ([Henneman et al., 2019b](#); [Casey et al., 2020](#)). Retaining individual links between interventional units and outcome units in T is differentiating priority of the methodology pursued here.

3.3 Indexing Potential Outcomes with Treatment Functions on the Bipartite Network

The bipartite setting’s lack of immediate correspondence between a single well-defined treatment for each outcome unit complicates the definition of relevant potential outcomes and causal contrasts above and beyond the difficulty in managing the sheer number of relevant potential outcomes. For example, while the approach of [Forastiere et al. \(2020\)](#) relied on delineation of the individual (and its treatment) and that individual’s neighbors (and their treatments) to define potential outcomes and formulate assumptions about interference, the bipartite setting entails no such natural notion of an “individual” treatment, since no treatment is directly applied to or withheld from the outcome units.

The approach here is to first identify a single interventional unit that might be particularly relevant for each outcome unit, and then follow similar reasoning to that outlined in

[Forastiere et al. \(2020\)](#) and [Karwa and Aioldi \(2018\)](#) for the case of a network or graph defined on one type of observational unit. The combination of these two strategies in the bipartite setting will support definition of functions of treatments on the network to encode assumptions about the interference in order to: a) reduce the number of potential outcomes required to answer relevant scientific questions and b) define causal estimands that can provide answers to those questions. This has been referred, as in [Karwa and Aioldi \(2018\)](#), as specifying an “exposure model” to specify how the treatments of those in the interference set impact outcomes of an index unit, and is similar to the “exposure mapping” of [Aronow and Samii \(2017\)](#). Definition and interpretation of the estimands described in the subsequent will rely heavily on assumptions about how the structure of interference matters (or not) for defining potential outcomes, that is, on the assumed “exposure model.” Given the importance of such assumptions, the ability to inform them with understanding of the physical process dictating the interference mechanism highlights an important distinction between studies of network treatment diffusion governed by complex exposure patterns and studies of social networks. In a social network context, the network structure is typically part of the data collection process; network ties are recorded based on an explicit criterion for connection between units. For example, two people are connected in the network if they report being friends. As a consequence, difficulties in defining and measuring connections, which may have implications for downstream analysis, can be considered as inherent features of the data collection process. In contrast, studies of network treatment diffusion specify a (physical or statistical) model for the network connections. Thus, any deficiency in the characterization of network connections is not part of data collection, but rather the specification for the mechanism generating interference. This highlights the importance of incorporating, when available, extant knowledge of the physical dynamics generating complex exposure dependencies. The threat of downstream analysis bias should be judged against the relative understanding of any supposed process dynamics.

In the bipartite context, [Zigler and Papadogeorgou \(2020\)](#) introduced the notion of a “key associated” interventional unit for each outcome unit in the bipartite network, that is, a 1:many mapping of interventional units to the outcome units. Specifically, denote with $j_{(i)}^*$ the interventional unit that is key-associated to the i^{th} outcome unit, for $i = 1, 2, \dots, n$. For the present investigation, $j_{(i)}^*$ will be the power plant that is most influential (as determined by HyADS) for the i^{th} ZIP code (specific definition deferred until Section 5). With definition of the key-associated unit, we define the key-associated treatment variable for each outcome unit, $Z_i = S_{j_{(i)}^*}$, pertaining to the intervention status of the key-associated interventional unit. For example, in the power plant investigation, Z_i will denote whether the power plant most influential for the i^{th} ZIP code had a scrubber installed for at least half of 2005. Note

that, in general, the definition of the key associated interventional unit for the i^{th} outcome unit need not be a function of T . For example, $j_{(i)}^*$ could be alternatively defined as the power plant that is geographically closest to the i^{th} ZIP code.

While interventions at the key-associated interventional units may be of particular interest, the presence of interference implies that outcomes at outcome unit i may additionally depend on interventions applied at units other than $j_{(i)}^*$. To reflect the additional dependence of potential outcomes on treatments applied at interventional units other than $j_{(i)}^*$, we introduce another treatment variable characterizing the treatments assigned at other units, in accordance with the information contained in the interference mapping T . Formally, let $g_i(\cdot; T) : \{0, 1\}^{J-1} \rightarrow \mathcal{G}_i$ be an exposure mapping function that maps, for a given interference mapping, T , the treatments on all J interventional units but the $j_{(i)}^{th}$ into a scalar value defined for each outcome unit $i = 1, 2, \dots, n$. Denote with G_i the value of the function $g_i(\mathbf{S}, T)$ for the i^{th} outcome unit. For example, the power plant investigation will make use of $G_i = c \sum_{j \neq j_{(i)}^*} t_{ij} S_j$ to denote the interference-weighted sum of scrubber installations to interventional units other than the key-associated unit, re-scaled by a constant c . While this quantity is closely related to the “neighborhood treatment” function defined in [Forastiere et al. \(2020\)](#), we will refer to this function as the “upwind treatment,” corresponding to its (approximate) interpretation in the evaluation of power plant interventions (where the term “upwind” is used loosely to reflect the information output by HyADS). A more general term relevant to other settings where interference is due to complex exposure patterns may be “upstream treatment”, because G_i is usually defined by weighting the treatment vector \mathbf{S} by the inward link weights t_i of the adjacency matrix T . It is worth stressing that, while in [Forastiere et al. \(2020\)](#) G_i is defined only on the treatment vector of the neighborhood of unit i , with neighbors being the nodes with a direct link to i on a one-mode network, in a bipartite setting G_i is a function of the whole treatment vector defined at the interventional-level. In fact, there is no notion of path distance in a bipartite network (unless it is projected to a one-mode set) and, hence, we do not need to make an assumption on the path order of interference. In principle, every power plant can have nonzero connection to every zipcode, with the extent of interference based on a physical model.

The utility of formulating the key-associated treatment, Z_i , and the upwind treatment, G_i , is that doing so permits a key assumption about potential outcomes that formalizes interference in the bipartite setting. Specifically, we adopt the following as an alternative to SUTVA in the case of bipartite causal inference with interference:

Assumption 1 (Upwind Interference). *For a fixed T , any two $(\mathbf{S}, \mathbf{S}') \in \mathcal{S}(J)$ such that the*

corresponding $Z_i = Z'_i$ and $G_i = G'_i$ yield the following equality:

$$Y_i(\mathbf{S}) = Y_i(Z_i, G_i) = Y_i(Z'_i, G'_i) = Y_i(\mathbf{S}')$$

In other words, Assumption 1 reduces the implications of interference to depend only on the index outcome unit's key-associated treatment and the scalar-valued function of treatments applied to all other interventional units. In the power plant example, this implies that the IHD hospitalization rate at ZIP code i would be the same under any two allocations of scrubbers to all power plants across the country that produces a specified treatment status of the most influential plant and the same upwind treatment rate.

As a consequence of Assumption 1, each outcome unit can be regarded as receiving a “treatment” that is dictated jointly by two components, Z_i and G_i . The assignment to Z_i is governed by the process that dictates whether the interventional units that are key associated to any outcome unit adopt treatment. The assignment to G_i is governed by the combination of the process that dictates whether *any* interventional unit adopts treatment and the structure of the interference network specified in T . This leads to formalization of an assignment mechanism governing the joint treatment, denoted with

$$P(\mathbf{Z}, \mathbf{G} | \mathbf{X}^{out}, \mathbf{X}^{int}, \{\mathbf{Y}(z, g), z \in \{0, 1\}, g \in \mathcal{G}\}), \quad (1)$$

where $g \in \mathcal{G}$ is, in a slight abuse of notation, taken to denote the values of g that are contained in \mathcal{G}_i for all i . Forastiere et al. (2020) formulated a similar assignment mechanism in the case of one level of observational unit, but in a setting where \mathbf{Z} and \mathbf{G} were deterministically linked for a fixed T . In contrast, the assignment mechanism in (1) permits independent variation in the two components of treatment, even for a fixed T . This results from the fact that the vector \mathbf{Z} encodes the treatment statuses of only the interventional units that are key-associated to at least one outcome unit (i.e., the elements of \mathbf{S} corresponding to $\{j_{(i)}^*; i = 1, 2, \dots, n\}$), whereas \mathbf{G} derives from the entire vector \mathbf{S} . Thus, insofar as there are elements of \mathbf{S} contained in the calculation of \mathbf{G} but not represented in \mathbf{Z} , it is possible, for a fixed T , for two different vectors of allocations to the interventional units, \mathbf{S}, \mathbf{S}' , to yield the same value of \mathbf{Z} , but different values of \mathbf{G} . As a consequence, it is possible (and indeed relevant in the power plant analysis) to conceive of interventions that would vary the value of \mathbf{G} without changing the value of \mathbf{Z} . This decoupling of \mathbf{Z}, \mathbf{G} in the assignment mechanism has important implications for the interpretation of the causal estimands that will be presented in Section 3.4.

3.4 Key-Associated Bipartite Causal Estimands

We define two causal estimands of interest that are anchored to the above definition of Z_i and G_i , both motivated by common notions of “direct” and “indirect” effects pertaining to the effect of treating an individual unit and the effect of treating “other” units. In the general bipartite setting, the lack of immediate delineation of which treatment applies “directly” to an outcome unit complicates the definition and meaning of such effects, but with the simplifications described in Section 3.1, “direct” will be used in reference to the key associated unit, and “indirect” or “upwind” used in reference to all other units.

We begin by defining average potential outcomes under particular values of the Z and G with:

$$\mu(z, g) = E[Y_i(Z_i = z, G_i = g)] \quad (2)$$

to denote expected value of the potential outcome for the i^{th} outcome unit when the upwind treatment takes the value g and the key-associated interventional unit has treatment z . Note that, considering the expectation over all i in 2 implicitly assumes that the value $Y_i(Z_i = z, G_i = g)$ is well defined for all outcome units. We continue development under this assumption for ease of exposition and because the interference process considered in the power plant example supports this assumption, but note that [Forastiere et al. \(2020\)](#) explicitly considers the possibility that the structure of the network would render certain values of G_i impossible for some i .

Using the above notation for the average potential outcome, we first define an estimand akin to an average “direct effect” of treating the key associated unit while holding fixed the treatments of other units:

$$\tau(g) = \mu(1, g) - \mu(0, g) \quad (3)$$

which might correspond, for example, to the average effect on IHD hospitalizations of installing (vs. not) a scrubber on the most influential power plant, while holding fixed the scrubber statuses of all upwind plants. An average direct effect over the distribution of G can be defined with $\tau = \sum_{g \in \mathcal{G}} \tau(g) P(G_i = g)$, where $\mathcal{G} = \cup_i \mathcal{G}_i$.

Another estimand, akin to an “indirect” or “spillover” effect, can be defined as:

$$\delta(g; z) = \mu(z, g) - \mu(z, 0) \quad (4)$$

to denote the average effect of changing the treatment statuses of interventional units in the interference mapping to toggle the “upwind” treatment from g to 0. In keeping with the

interpretation of the power plant example, we will refer to this effect as the “upwind” effect, interpretable as the average effect on IHD hospitalizations of having upwind scrubber rate g relative to having no scrubbers located upwind, while holding fixed the scrubber status of the most influential plant at z . An average upwind effect over the distribution of G can be defined as $\Delta(z) = \sum_{g \in \mathcal{G}} \delta(g; z) P(G_i = g)$. Note that versions of upwind effects could be defined to compare any two g, g' , and not just g to 0.

The estimands in (3) and (4) are based on setting both the treatment of the key associated interventional unit and the treatments of interventional units in the interference mapping. Average direct and upwind effects are then calculated according to the (empirical) distribution of $P(G_i = g)$. These average estimands are similar to the ones introduced in [Forastiere et al. \(2020\)](#), and isolate the effect of a specific intervention from the effect of changing the distribution of the treatment in the population (see [Forastiere et al. \(2020\)](#), Section 2.4, for a discussion). This stands in contrast to other work that defines average effects over hypothetical interventions on the whole sample, (e.g. general stochastic interventions in [Van der Laan \(2014\)](#) and its extensions or Bernoulli trials in [Liu et al. \(2016\)](#)).

3.5 Ignorable Treatment Assignment

With the bivariate treatment formulated above and the corresponding joint treatment assignment mechanism, identification of causal effects relies on an assumed version of ignorable treatment assignment

Assumption 2 (Ignorability of Joint Treatment Assignment).

$$Y_i(z, g) \perp\!\!\!\perp Z_i, G_i \mid \{\mathbf{X}_j^{int}\}_{j \in t_i^\top}, \mathbf{X}_i^{out} \quad \forall z \in \{0, 1\}, g \in \mathcal{G}_i, \forall i.$$

This assumption states that the treatment status of an outcome unit’s key-associated interventional unit and that outcome unit’s upwind treatment are independent of the potential outcomes, conditional on the covariates for the interventional units in the i^{th} unit’s interference set ($\{\mathbf{X}_j^{int}\}_{j \in t_i^\top}$) and the covariates of the outcome unit (\mathbf{X}_i^{out}).

The set of interventional-level covariates in $\{\mathbf{X}_j^{int}\}_{j \in t_i^\top}$ includes the vector of covariates for the key-associated unit, $\mathbf{X}_{j_{(i)}^*}^{int}$, but it may also include functions of the covariate values of other interventional units in the interference set, perhaps calculated with the same $g(\cdot)$ used to define the upwind treatment. For example, one might include within $\{\mathbf{X}_j^{int}\}_{j \in t_i^\top}$ the HyADS-weighted average size of plants upwind of ZIP code i , not including power plant $j_{(i)}^*$.

The set of confounders $\{\mathbf{X}_j^{int}\}_{j \in t_i^\top}$ and \mathbf{X}_i^{out} that should be conditioned on to satisfy Assumption 2 include all those covariates that affect either Z_i or G_i and the outcome $Y_i(z, g)$. One might question why outcome unit covariates should dictate treatments adopted at interventional units and why interventional unit covariates should relate to outcomes measured at outcome units. This is a distinct feature of the bipartite setting, and relates to the specification of the interference mapping, T . Due to the specification of links in T , outcome-unit covariates in \mathbf{X}_i^{out} could relate to the likelihood of the treatment for the associated interventional units (Z_i and G_i) if those treatment decisions are based in part on knowledge of the linked outcome units. For example, in the power plant setting, decisions to install scrubbers may be based in part on knowledge of downwind population centers or particular areas cited for regulatory noncompliance. Similarly, interventional-unit covariates in $\{\mathbf{X}_j^{int}\}_{j \in t_i^\top}$ could relate to outcomes if certain types of interventional units tend to be linked with certain types of outcome units. For example, larger power plants with higher propensity to install scrubbers may tend to be located nearer to large population centers exhibiting particular patterns in hospitalization rates.

The dependent network and spatial structure of the bipartite problem warrants further consideration. In traditional social networks, the threat of confounding can arise due to homophily, that is, the tendency of nodes with similar features to share edges. The closest analogue in the bipartite setting is outcome units with similar features tending to share connections with similar sets of interventional units. In the power plant study, this would correspond to ZIP codes with similar features tending to share influence from similar sets of power plants. This can arise when ZIP codes that are geographically close share influence with the same set of (upwind) power plants. The threat of confounding due to this type of homophily can be mitigated by a) including appropriate covariates in X_i^{out} (for example, many demographic and meteorological factors measured at each ZIP in the power plant analysis) and b) recognition of whether the underlying reasons for shared edges in the interference network are fully specified (e.g., as in a physical process with the HyADS model), and thus not a consequence of unobserved similarities among units that often threaten the validity of studies of social networks. Another potential violation of the ignorability assumption relates to the spatial correlation of outcome unit potential outcomes which. While not generally the same as homophily, such correlation is likely related in the power plant case due to the similarity of ZIP codes that are spatially close. In particular, the spatial nature of G_i could imply that its value for an index ZIP code is related to the potential outcomes of nearby ZIP codes which, when potential outcomes are spatially correlated, could yield confounding due to outcomes at nearby ZIP codes being jointly associated with $Y_i(z, g)$ and G_i . This threat is mitigated in the power plant analysis for two distinct reasons. First is the inclusion of

many covariates in \mathbf{X} that are themselves spatially correlated in accordance with the spatial patterning of IHD admissions, thus reducing the possibility of nearby IHD hospitalizations being conditionally associated with those at ZIP code i . Second, the nature of the upwind treatment, G_i , is dictated primarily by wind patterns, presenting the plausible argument that variability in G_i does not systematically align with the (conditional) spatial correlation of potential IHD hospitalizations. These are both distinct phenomena from those that could arise in settings where interference arises due to unit-to-unit outcome dependencies; in the power plant setting, spatial correlation in potential outcomes does not result from dependencies in outcomes among neighboring areas. We revisit the specific interventional and outcome unit covariates used in the power plant analysis in Section 5.

In combination with the assumption of consistency, Assumptions 1 and 2 support identification of the causal effects from Section 3.4 with observed data. In addition, we adopt a version of the positivity assumption that the joint treatment probability in (1) is strictly between 0 and 1, that is, there is no combination of $\mathbf{X}_i^{out}, \{\mathbf{X}_j^{int}\}_{j \in t_i^{\perp}}$ that deterministically dictates the individual or upwind treatment, which is of practical importance when confronting issues of in-sample overlap between the covariate distributions of units with different levels of the observed key-assocaited and upwind treatment. Arguments for identification in this case follow those provided in [Forastiere et al. \(2020\)](#).

4 Estimating Bipartite Causal Effects with Joint Propensity Scores

For estimating the causal effects defined in Section 3.4, we adopt an estimation approach similar to that in [Forastiere et al. \(2020\)](#), which estimates a joint propensity score derived from the assignment mechanism in (1) and deploys joint propensity score estimates in a manner similar to how propensity scores have been previously adopted to adjust for confounding in observational studies ([Rosenbaum and Rubin, 1983](#); [Imbens, 2000](#); [Hirano and Imbens, 2004](#); [Stuart, 2010](#)).

4.1 Specification of the Joint Propensity Score

The *joint propensity score* governing the assignment of the key-associated and upwind treatments can be denoted as

$$\psi(z, g; x^{int}, x^{out}) = P(Z_i = z, G_i = g | \mathbf{X}_{j_{(i)}^*}^{int} = x^{int}, \mathbf{X}_i^{out} = x^{out}) \quad (5)$$

[Forastiere et al. \(2020\)](#) established the balancing score property of a joint propensity score such as this, indicating that, when adjustment for $\mathbf{X}_{j_{(i)}^*}^{int}$ and \mathbf{X}_i^{out} is sufficient to control for confounding, so is adjustment for $\psi(z, g; x^{int}, x^{out})$. Specifically, [Forastiere et al. \(2020\)](#) show that, under the previously-stated assumptions, average potential outcomes in (2) can be estimated as functions of observed data of the form $E[E[Y_i | Z_i = z, G_i = g, \psi(z, g; x^{int}, x^{out})] | Z_i = z, G_i = g]$, representing the average of observed outcomes under $Z = z$ and $G = g$ for observations with the same value of the joint propensity score, averaged again over the empirical distribution of the joint propensity score. As a practical matter, the multi-valued nature of the joint treatment (owing to the scale of the upwind treatment, G) makes direct adjustment for $\psi(z, g; x^{int}, x^{out})$ difficult. However, the binary nature of the key-associated treatment motivates the following factorization of the joint propensity score:

$$\begin{aligned} \psi(z, g; x^{int}, x^{out}) = & P(Z_i = z, G_i = g | \mathbf{X}_{j_{(i)}^*}^{int} = x^{int}, \mathbf{X}_i = x^{out}) = \\ & P(G_i = g | Z_i = z, \mathbf{X}_{j_{(i)}^*}^{int,g} = x^{int,g}, \mathbf{X}_i^{out,g} = x^{out,g}) \times \end{aligned} \quad (6)$$

$$P(Z_i = z | \mathbf{X}_{j_{(i)}^*}^{int,z} = x^{int,z}, \mathbf{X}_i^{out,z} = x^{out,z}) \quad (7)$$

where we denote the part of the factorization in (6) with $\lambda(g; z, x^{int,g}, x^{out,g})$ to represent the probability of having upwind treatment level g conditional on z and covariates, and we denote the part of the factorization in (7) with $\phi(z; x^{int,z}, x^{out,z})$ to denote the probability of having the key-associated treatment at level z , conditional on covariates. Note the expanded notation to reflect the possibility of refining the model specification with the assumption that these two components of the joint propensity score model might not include the same covariates; $\mathbf{X}^{out,g}$ represents the outcome-unit covariates relevant to the assignment of G and $\mathbf{X}^{out,z}$ represent the outcome-unit covariates relevant to the assignment of Z , with analogous definitions for $\mathbf{X}^{int,g}$ and $\mathbf{X}^{int,z}$. The binary nature of the key-associated treatment, Z (relating to $\phi(z; x^{int,z}, x^{out,z})$), supports the use of techniques common to the literature on propensity score adjustment for binary treatments, while the continuous domain of the upwind treatment, G (relating to $\lambda(g; z, x^{int,g}, x^{out,g})$), can be viewed in the way generalized propensity scores have been proposed in the context of continuous treatments ([Hirano and](#)

Imbens, 2004).

4.2 Estimating Procedure: Subclassification and Generalized Propensity Score Adjustment

We outline one approach for confounding adjustment with the joint propensity score that unfolds in two steps. The first step estimates the key-associated propensity score $\phi(z; x^{int,z}, x^{out,z})$ for every outcome unit and then stratifies all units into K subclasses, each having roughly homogeneous distributions of the key-associated propensity score. Then, within each subclass, the upwind propensity score is estimated and then used in a model-based approach for confounding adjustment. Note this represents but one of many possible ways that estimates of the joint propensity score could be obtained and used for confounding adjustment.

Estimates of the key-associated propensity score, $\phi(z; x^{int,z}, x^{out,z})$ are obtained from a model of the form $P(Z_i = z | \mathbf{X}_{j_{(i)}^*}^{int,z}, \mathbf{X}_i^{out,z}) = f^Z(z, \mathbf{X}_{j_{(i)}^*}^{int,z}, \mathbf{X}_i^{out,z}; \gamma)$, with predicted values from this model, denoted with $\hat{\phi}_i$ for each of $i = 1, 2, \dots, n$. Each of the n outcome units is then assigned to one of K strata, denoted K_1, K_2, \dots, K_K , based, for example, on quantiles of the $\hat{\phi}_i$. The covariates $\mathbf{X}^{int,z}, \mathbf{X}^{out,z}$ should be balanced between units with $Z = 0$ and those with $Z = 1$ within each of the K strata, which can be checked empirically.

Within each of the K strata, we estimate a parametric dose-response function for the potential outcomes, $\mu_k(z, g) = E[Y_i(Z_i = z, G_i = g) | i \in K_k]$. This is accomplished by first estimating a parametric model for the upwind propensity score, $\lambda(g; z, x^{int,g}, x^{out,g})$ within the stratum, specified as $P(G_i = g | Z_i = z, \mathbf{X}_i^{int,g}, \mathbf{X}_i^{out,g}) = f^G(g, z, \mathbf{X}_i^{int,g}, \mathbf{X}_i^{out,g}; \delta^k)$, where the parameters indexing this model, δ^k , are allowed to differ across the K subclasses. Density estimates from this model, denoted with $\hat{\lambda}_i$, are estimates of the upwind propensity score. The observed data within each of the K strata are then used to estimate a model for the potential outcomes $Y_i(z, g) | \hat{\lambda}_i \sim f^y(z, g, \hat{\lambda}; \theta_k)$. Predicted values from this model, denoted with $\hat{Y}_i(z, g)$, represent estimated potential outcomes for every level of $(Z_i = z, G_i = g)$ across a pre-defined grid of values. The estimated within-stratum dose-response function $\mu_k(z, g)$ is then obtained by averaging these predicted potential outcomes for each value of (z, g) as:

$$\hat{\mu}_k(z, g) = \frac{\sum_{i \in n_k} \hat{Y}_i(z, g)}{n_k}.$$

These within-stratum dose-response functions are then averaged over the K strata to obtain an overall estimate with $\hat{\mu}(z, g) = \sum_{k=1}^K \hat{\mu}_k(z, g) \pi^g$, where π^g denotes the proportion of

observations observed to lie in stratum K_k . Estimates of $\hat{\mu}(z, g)$ are then used to obtain estimates of the causal estimands defined in Section 3.4.

For inference, we adopt the bootstrap approach used in [Forastiere et al. \(2020\)](#) that is motivated by an “egocentric” network sampling mechanism where independent samples of outcome units are drawn with replacement, but the structure of the entire network is preserved in that each outcome unit’s key-associated unit ($j_{(i)}^*$), key-associated treatment, covariates, and upwind treatment ($Z_i, \mathbf{X}_i^{int}, \mathbf{X}_i^{out}, G_i$) are regarded as node characteristics that do not change across bootstrap samples. To the extent that this assumed egocentric bootstrap sampling does not correspond to how the data (e.g., in the power plant investigation) were actually sampled, the validity of the bootstrapped variance estimates is not guaranteed. Nonetheless, [Forastiere et al. \(2020\)](#) showed via a simulation study that, in the setting of one level of observational unit outcome that are not correlated, this variance estimate, while not ideal, produces variance estimates that are consistent with monte carlo variability in point estimates and represent a reasonable approximation.

5 Evaluating the Effectiveness of scrubbers for reducing Medicare IHD Hospitalization

We deploy the HyADS dispersion model and statistical methods described in the previous sections to evaluate the extent to which presence of scrubbers on coal-fired power plants in 2005 caused improvements in IHD hospitalizations among Medicare beneficiaries during that same year, accounting for the interference arising due to long-range pollution transport, as described in Section 2.

Specifically, the interventional units are $J = 472$ electricity generating facilities (“power plants”) operating in 2005 that use coal as the primary fuel, of which 106 had scrubbers installed ($S_j = 1$) during at least half of 2005. The HyADS approach of Section 2 was used to quantify the annual impact of air originating at each of the 472 facilities on each ZIP code in the US. For the analysis, $n = 23,675$ ZIP codes, lying mostly in the Eastern US (where most coal power plants are located) were retained on the basis of having an annual HyADS value in excess of the 25th percentile of the national distribution (that is, annual HyADS value greater than 181371.50) and meeting propensity score overlap criteria described later. Thus, the outcome units are these $n = 23,675$ ZIP codes where pollution from coal-fired power plants comprises an important feature of the ambient air quality. Figure 1 presents a map of these ZIP codes, which contain data on 22,603,597 fee-for-service Medicare beneficiaries

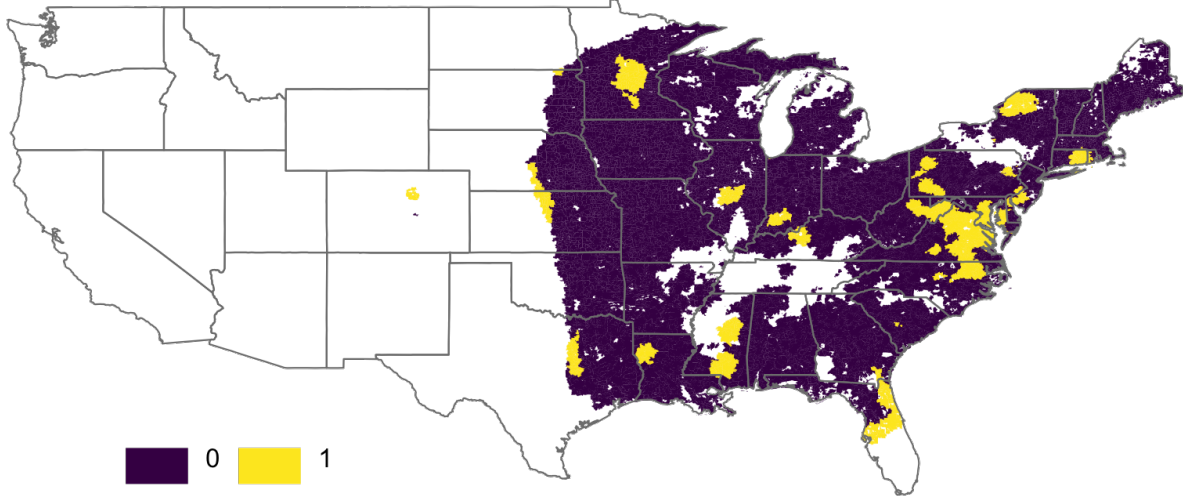


Figure 1: 23,675 ZIP codes subject to meaningful coal power plant pollution in 2005, colored according to whether the key-associated plant has a scrubber ($Z_i = 0$ or 1). White areas are omitted from the analysis because of low power plant exposure or lack of propensity score overlap.)

in 2005.

The same output from the HyADS simulations was used as the interference mapping, T . Specifically, let t_{ij} from Section 3.2 be the value from the source-receptor matrix output from HyADS denoting how much air mass originating at power plant j travels to ZIP code i . The key-associated plant for each ZIP code $i = 1, 2, \dots, 23,675$ was identified based on the plant exhibiting the highest HyADS influence on ZIP code i during 2005, that is, $j_{(i)}^*$ is the element of t_i with the highest value ($j; t_{ij} = \max_j \{t_{ij}\}$). In total, 275 of the 472 power plants were key-associated to at least one ZIP code, with 35 of these key-associated plants having scrubbers installed for at least half of 2005. This leads to a key-associated treatment, $Z_i = S_{j_{(i)}^*} = 1$ for 2,753 ZIP codes whose most influential power plant had a scrubber for at least half of 2005. Figure 1 denotes which locations have $Z_i = 1$.

As stated in Section 3.4, the upwind treatment, G_i for $i = 1, 2, \dots, 23,675$ is defined as a linear function of the treatment statuses of all power plants but power plant $j_{(i)}^*$, weighted by the elements of the interference mapping and rescaled by the maximum value to be between 0 and 1: $G_i^* = \sum_{j \neq j_{(i)}^*} t_{ij} S_j$, and $G_i = \frac{G_i^*}{\max_i(G_i)}$. Since t_{ij} , as output from HyADS, denotes

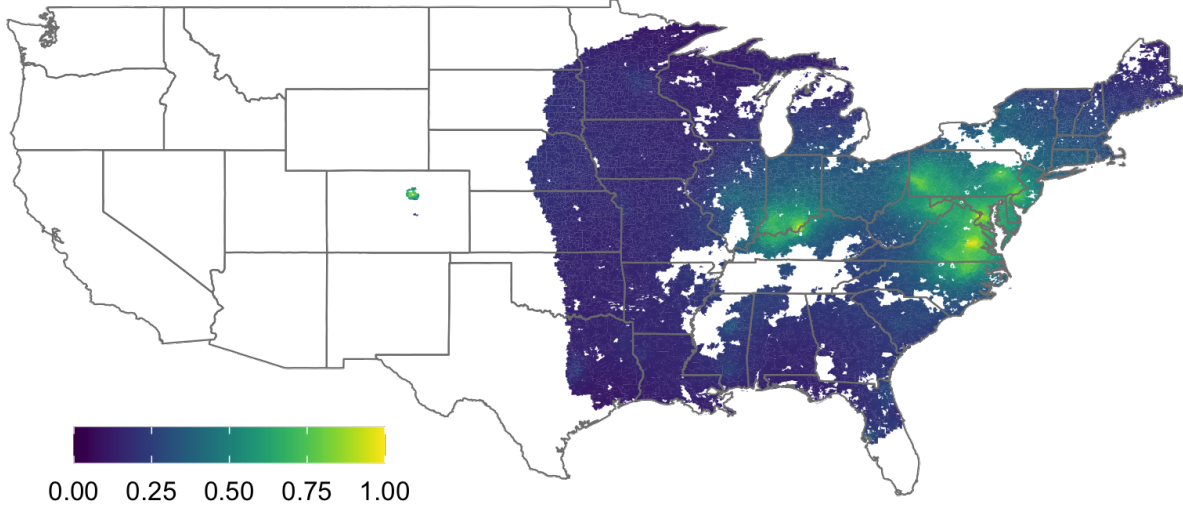


Figure 2: 23,675 ZIP codes subject to meaningful coal power plant pollution in 2005, colored according to the HyADS-weighted upwind treatment rate, G .)

the strength of influence of the j^{th} interventional unit on the i^{th} outcome unit, this function can be loosely interpreted as an “upwind weighted” rate of scrubbers among all but the key-associated power plant, so that a ZIP code can have high values of G_i if it is heavily exposed to emissions from many power plants with scrubbers or from a few very influential power plants with scrubbers (or both). Figure 2 maps the values of G_i across the study area.

5.1 Model specification for the joint propensity and potential outcomes

The covariates included in $\mathbf{X}_i^{int,z}, \mathbf{X}_i^{out,z}, \mathbf{X}_i^{int,g}, \mathbf{X}_i^{out,g}$ are listed and summarized in Table 1. Outcome-unit covariates \mathbf{X}_i^{out} include characteristics of the general population living in ZIP code i (e.g., population, population density, percent Hispanic, high school graduation rate, median household income, poverty, occupied housing, migration rate (% of residents who moved within 5 years), smoking rate), climatalogical factors (temperature and relative humidity), characteristics of the Medicare population living in the ZIP code (average age, percent female beneficiaries, percent white beneficiaries, and percent black beneficiaries), and general measure of power plant pollution in the area according to quartile of the overall

HyADS distribution. Interventional-unit covariates \mathbf{X}_j^{int} include characteristics of the power plants from 2005 such as the total number of controls for oxides of nitrogen (NO_x) emissions, the percent of units with Selective (non) Catalytic Reduction systems (a particular technology for NO_x control), total heat input, total operating time, the average percent of operating capacity, and whether the plant participated in Phase II of the ARP.

The model for the key-associated propensity score, $\phi(z; x^{int,z}, x^{out,z})$, specifies $f^Z(z, \mathbf{X}_{j_{(i)}^*}^{z,int}, \mathbf{X}_i^{z,out}; \gamma)$ as a logistic regression with main effect terms for each of $\mathbf{X}_{j_{(i)}^*}^{int,z}, \mathbf{X}_i^{out,z}$, denoting the each of the power plant characteristics (of the key-associated plant) and each of the ZIP code characteristics listed in Table 1. Estimates of this model are then used to group each of the $n = 23,675$ ZIP codes into one of $K = 5$ strata based on the quintiles of the distribution of $\hat{\phi}_i$ among the ZIP codes with $Z_i = 1$. Figure 3 depicts the standardized mean difference in each covariate before the stratification, within each of the K strata, and on average across all strata. Note that, while the average standardized mean covariate difference across all strata is generally reduced relative to the unadjusted differences, serious imbalance remains, in particular within individual propensity score strata, motivating the use of further covariate adjustment in addition to adjustment for $\hat{\phi}_i$, as will be described later.

Within each of the K strata, the model for the upwind propensity score, $\lambda(g; z, x^{int,g}, x^{out,g})$, specifies $f^G(g, z, \mathbf{X}_i^{int,g}, \mathbf{X}_i^{out,g}; \delta^k)$ as a normal regression model with linear main effect terms for only the ZIP code characteristics listed in Table 1 ($\mathbf{X}_i^{out,g}$).

The outcome model for estimating $E[Y_i(Z_i = z, G_i = g)|i \in K_k]$ specifies $f_k^y(z, g, \hat{\lambda}; \theta_k)$ as a Poisson regression of the form:

$$\log\left(\frac{Y_i(z, g)}{\text{Beneficiaries}_i}\right) = \beta_0 + \beta_z z + \beta_g g + \beta_\lambda \hat{\lambda}_i + \beta_X^\top \mathbf{X}_i^{out}$$

where Beneficiaries_i is the number of Medicare fee-for-service person-years at risk for ZIP code i in 2005 and \mathbf{X}_i^{out} contains all the ZIP code characteristics in Table 1 to adjust for residual confounding not captured by the key-associated propensity score subclassification.

5.2 Power Plant Analysis Results

An analysis with 500 bootstrap samples for standard error estimation estimates $\hat{\tau} = -7.95(-19.27, 3.50)$, indicating that, on average, having a scrubber installed on a ZIP code's most influential power plant causes a reduction approximately 8 hospitalizations per 10,000 person-years, although this estimate cannot be conclusively distinguished from zero. The upwind treatment effect

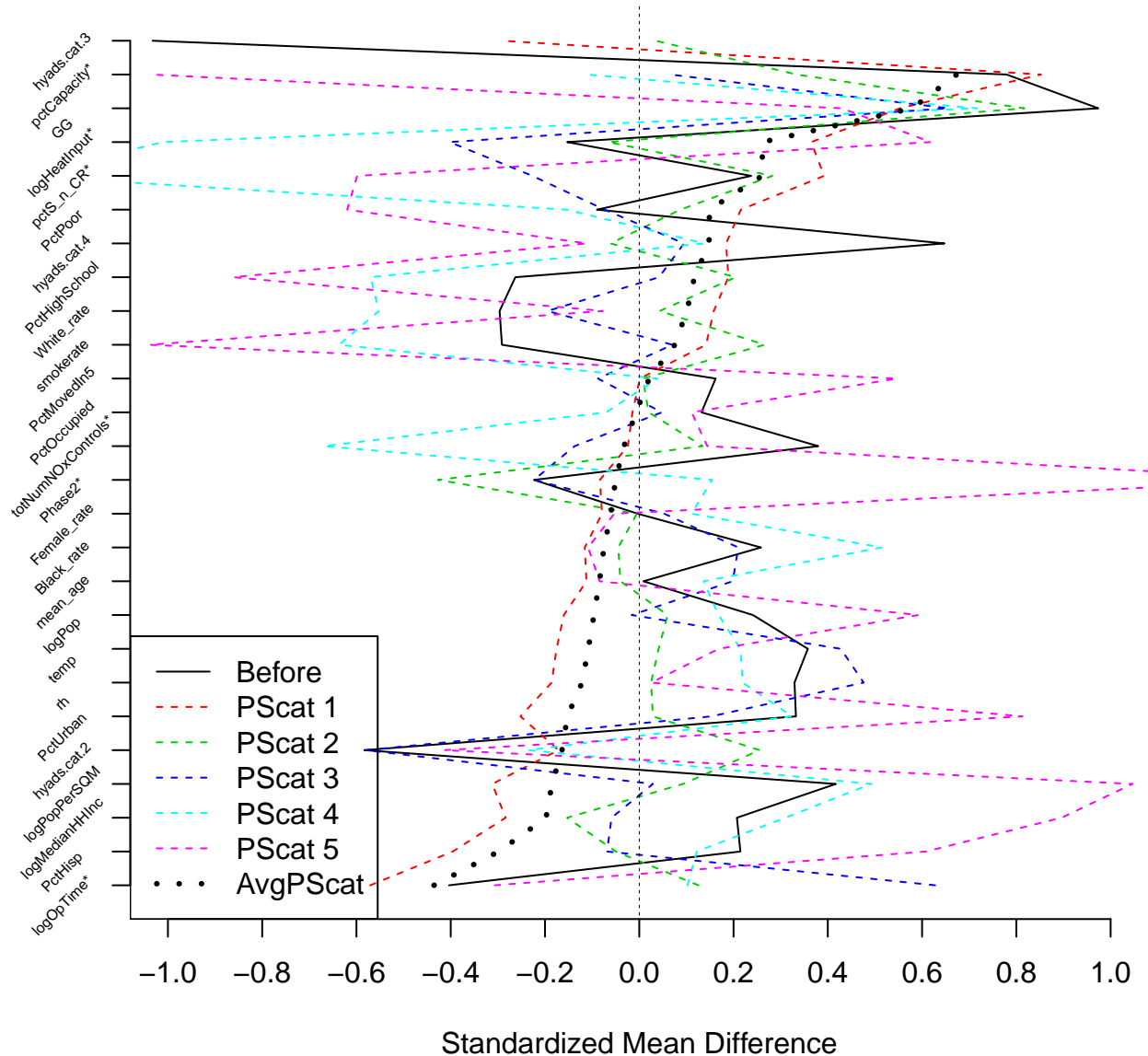


Figure 3: Balance Plot. Variables with * are individual power plant characteristics that are not likely confounders.

Table 1: Covariate summary across levels of the key-associated treatment, Z .

		Mean $Z=0$	Mean $Z=1$
ZIP Code Characteristics, \mathbf{X}^{out}	G	0.29	0.53
	log(population)	8.22	8.62
	% Urban	0.40	0.54
	% Hispanic	0.03	0.05
	% High School Grad	0.36	0.33
	log(MedianHouseholdIncome)	10.54	10.62
	% Poverty	0.12	0.11
	% Occupied Housing	0.88	0.89
	Migration Rate	0.41	0.44
	$\log(\frac{pop}{mi^2})$	5.02	5.87
	Smoking Rate	0.26	0.25
	Temperature	286.55	288.27
	Relative Humidity	0.01	0.01
	Age	74.97	74.99
	% Female	0.56	0.56
	% White	0.90	0.84
	% Black	0.08	0.13
	HyADS Category 2	0.27	0.10
HyADS Category 3	0.22	0.03	
HyADS Category 4	0.24	0.56	
Power Plant Characteristics, \mathbf{X}^{int}	Total NO_x Controls	4.12	5.49
	log(HeatInput)	14.91	14.77
	log(OperatingTime)	7.73	7.56
	% Operating Capacity	0.62	0.75
	% of Selective (non) Catalytic Reduction	0.17	0.27
	ARP Phase II	0.70	0.59

is estimated to be $\hat{\Delta}(0) = -15.08(-24.14, -6.28)$ among ZIP codes for which the most influential power plant is without scrubber, and $\hat{\Delta}(1) = -29.28(-50.09, -8.91)$ among the ZIP codes for which the most influential power plant has a scrubber. Figure 4 shows the estimated dose-response curves of $Y(z, g)$ against $g \in [0, 1]$ for $z = 0, 1$, indicating a clear trend that more upwind scrubbers are associated with lower IHD hospitalization rates, except possibly at the highest levels of g where there is substantial uncertainty in $Y(0, g)$ (owing to the relatively small number of zip codes with $Z_i = 0$ and high values of g) and an evident leveling off of the trend in $Y(1, g)$, suggesting that, at ZIP codes where the key-associated plant has a scrubber, reducing g from values near 0.5 offers similar benefit to reductions from higher levels of g .

For reference, we also conduct an analysis using the same model specification as de-

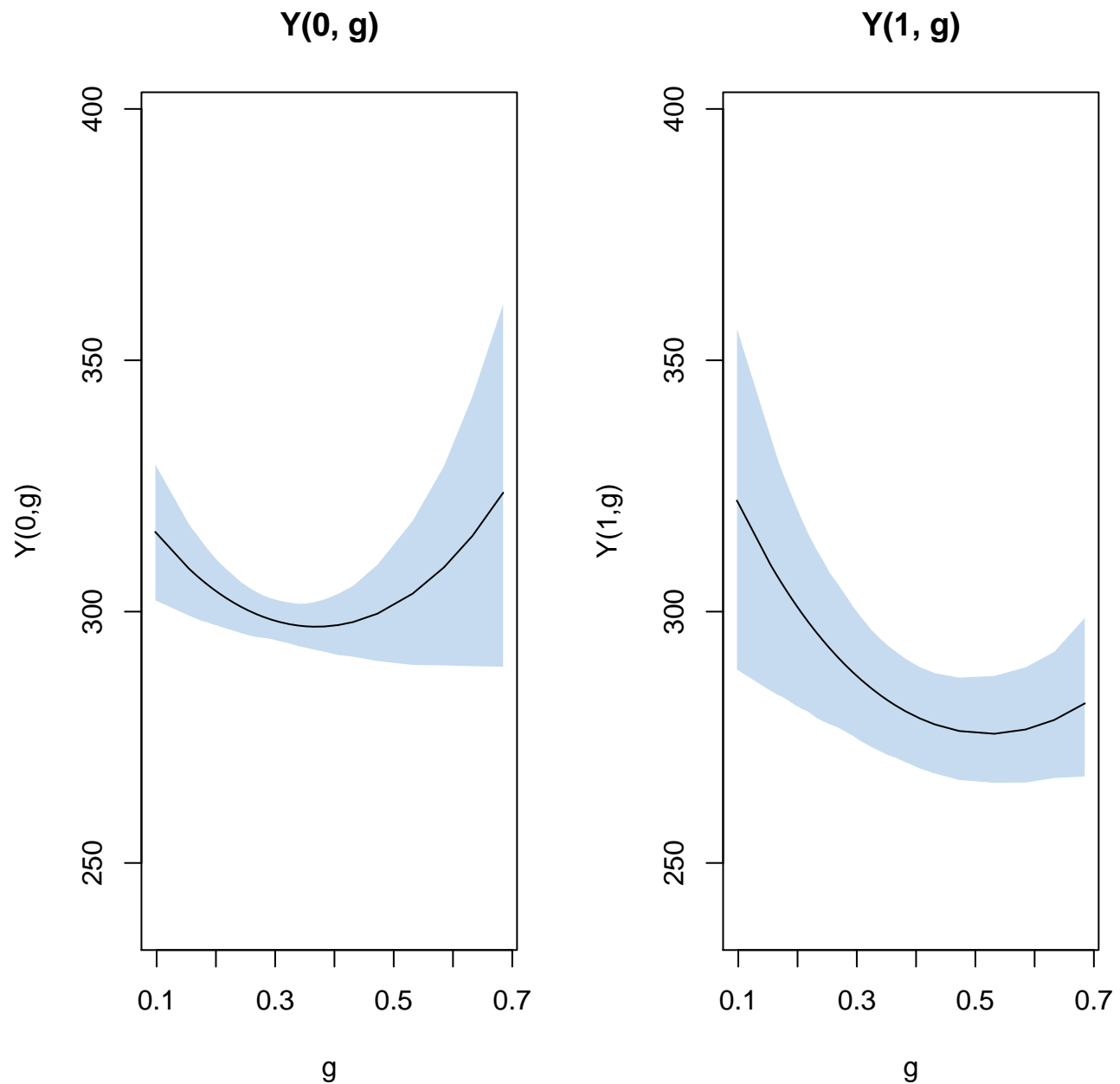


Figure 4: Estimated dose-response curves, where $Y(z, g)$ represents the Medicare IHD hospitalization rate per 10,000 person-years

scribed above, but with ambient $\text{PM}_{2.5}$ as the outcome and the outcome model within subclasses of key-associated propensity scores specified as a normal regression with mean expression analogous to the Poisson regression in Section 5.1. This analysis can be viewed as a rough validation of the IHD analysis, as the link between power plant pollution and ambient $\text{PM}_{2.5}$ is reasonably well understood, with a clear expectation that scrubbers reduce ambient $\text{PM}_{2.5}$ both locally and at downwind locations. This analysis yields estimates of $\hat{\tau} = -0.21(-0.33, -0.11)$; $\hat{\Delta}(0) = -0.28(-0.39, -0.19)$; $\hat{\Delta}(1) = -0.22(-0.43, -0.02)$, with depiction of the dose-response curves between g and $Y(z, g)$ for $z = 0, 1$ in Figure 5. Thus, the analysis strongly suggests that having a scrubber on the key-associated power plant reduces ambient $\text{PM}_{2.5}$ by approximately 0.2 micrograms per meter cubed ($\frac{\mu\text{g}}{\text{m}^3}$), with a clear signal that larger rates of upwind scrubbers lead to lower ambient $\text{PM}_{2.5}$. For reference, the federal ambient air quality standard for annual average $\text{PM}_{2.5}$ is 12 $\frac{\mu\text{g}}{\text{m}^3}$, and a reduction of 0.2 $\frac{\mu\text{g}}{\text{m}^3}$ attributable to any single source is substantial.

6 Discussion

We have offered new estimands and a corresponding estimation strategy for causal effects on a bipartite network. The investigation was specifically motivated by a problem in air pollution regulatory policy where scrubbers installed at coal-fired power plants are investigated for their effectiveness for reducing Medicare IHD hospitalizations, but hold relevance for other types of policies or interventions where the units on which the treatments are defined (here, coal-fired power plants) are distinct from the units on which outcomes are relevant (here, ZIP codes), and the complex nature of relationships between these distinct types of unit lead to interference. While the strategy has close ties to that recently proposed in [Forastiere et al. \(2020\)](#), deploying this type of methodology in the setting of a bipartite network where interference arises due to a complex physical process entailed several distinctions and extensions over the more typical analysis of a social network.

First, the bipartite nature of the problem complicates standard notions of “direct,” “indirect,” and “spillover,” since there is no immediate correspondence governing which interventions apply “directly” or “indirectly” to an outcome unit. The approach here provided a set of estimands that rely on specification of a key-associated interventional unit for each outcome unit, representing a subset of bipartite estimands proposed in [Zigler and Papadogeorgou \(2020\)](#) that hold particular relevance in the power plant investigation. Relying on the notion of the key-associated and upwind treatments in the bipartite setting introduced further differentiation with the work in [Forastiere et al. \(2020\)](#). For example, this formulation

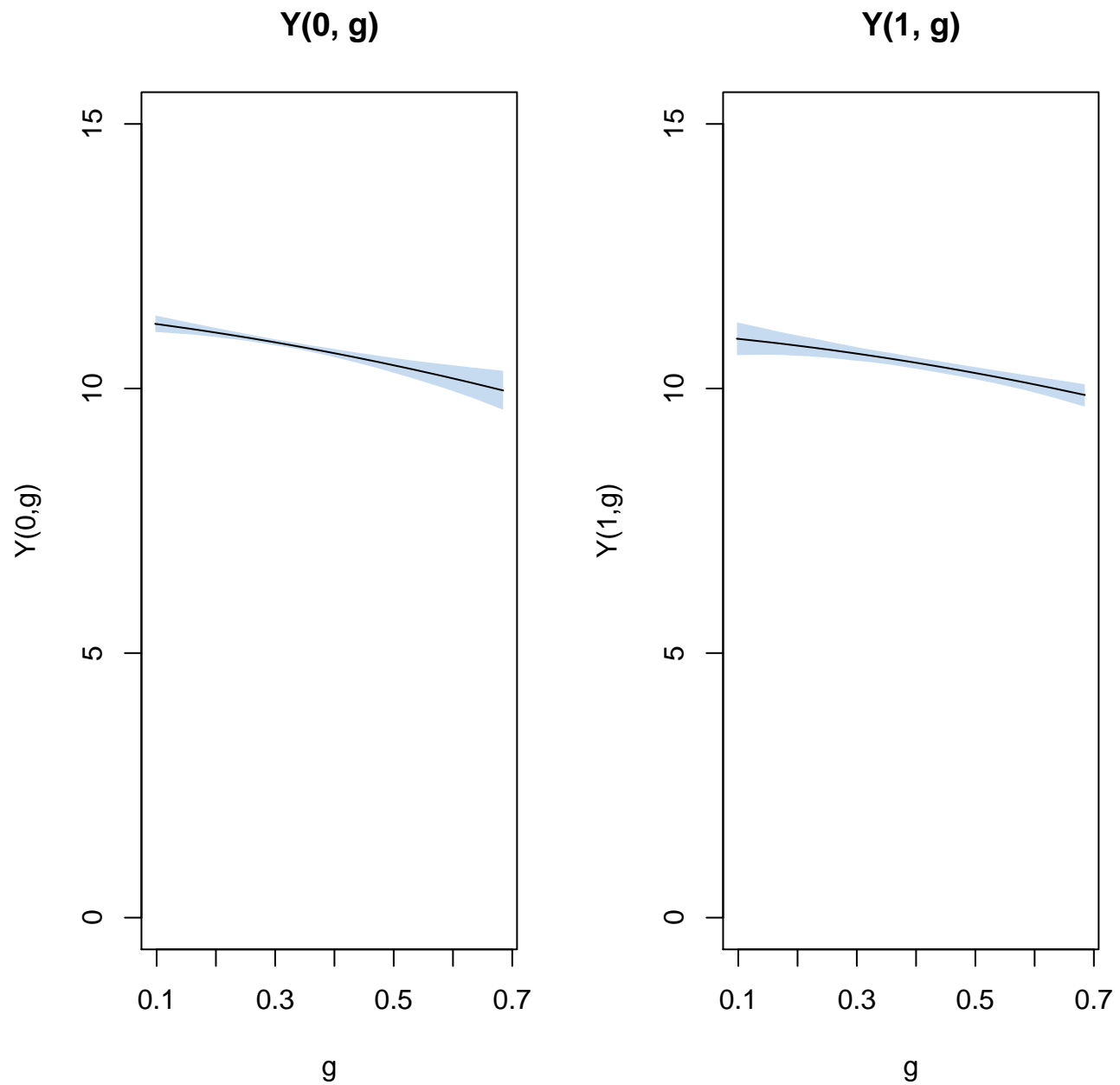


Figure 5: Estimated dose-response curves for the analysis where $Y(z, g)$ represents $\frac{\mu\text{g}}{\text{m}^3}$ of ambient $\text{PM}_{2.5}$.

presented the possibility of a joint assignment mechanism (for Z and G) that naturally corresponds to independent variability in the two treatment components, even for a fixed network. This is an important distinction with similar approaches in the setting with one level of observational unit, where “neighborhood” treatments analogous to G would be deterministically governed by the structure of the network, T , and the allocation of treatments to individual units, Z . Thus, in the bipartite setting, the indirect effect proposed in Section 3.4 might correspond more naturally to an actual and implementable intervention that changes allocations to some interventional units (and, as a consequence, the level of G) without changing Z . These features are in part a consequence of the fact that the type of interference considered here is that due to complex exposure patterns, which is an important distinction with most existing work where interference arises from unit-to-unit outcome dependencies. This was framed as a problem of interference on a weighted, directed network, expanding common notions of network dependency and adjacency that arise in settings where interference arises due to outcome dependence among one level of observational unit. Issues related to spatial correlation, homophily, and confounding all take on somewhat different meanings than those that have become routine in studies of adjacency networks. More broadly, the particulars of the power plant investigation anchored the deployment of causal inference methods to confront interference with data that are explicitly spatially-indexed. Despite early progress in [Verbitsky-Savitz and Raudenbush \(2012\)](#) and attempts in [Giffin et al. \(2020\)](#), the literature on explicit and potential-outcomes based methods for spatial interference remains sparse.

In addition to the contributions to statistical methodology, this work represents the first (to our knowledge) rigorous application of methods for causal inference with interference in air pollution that attempts to reflect the complex atmospheric processes underlying the interference. A previous analysis in [Zigler and Papadogeorgou \(2020\)](#) relied on ad-hoc clustering, which was known to be a gross simplification of interference in this context. The combination of the data sources described in Section 2 with the novel reduced-complexity atmospheric model (HyADS) to characterize the structure of interference represents an important advance in environmental data science at the intersection of statistics and atmospheric science. What’s more, the formalization of potential outcomes to focus on causal estimands indexed by discrete interventions at power plants (i.e., the installation or not of a scrubber) and acknowledge interference is an important advance over previous epidemiological investigations that deploy HyADS to characterize locations’ cumulative exposure to a set of power plants, without maintaining the explicit distinction between which of a set of power plants did or did not take a particular action ([Henneman et al., 2019b](#)). The explicit link to well-defined interventions can lead to arguably more policy-relevant evidence to guide future policy actions.

Despite the advances in methods for causal inference and analysis of air quality policy, there are important limitations to this work. First is the bootstrap method used for inference, which is only strictly valid under a specific sampling scheme that does not correspond to how the power plant data were sampled. The approach here is expected to yield a reasonable approximation, but further work on inference in this type of network is clearly warranted. Such development should include work to formalize “design-based” standard errors acknowledging that error in this case where nearly the entire population of relevant power plants and ZIP codes is observed, derives from the assignment to treatments and not standard notions of sampling variability (Abadie et al., 2019). Second, the estimation strategy of first stratifying outcome units on the key-associated propensity score and then fitting parametric models within strata for the upwind propensity score and the potential outcomes represents one reasonable approach, but the threat of confounding remained particularly pronounced in the lack of covariate balance for many ZIP code features within subclasses of the key-associated propensity score, with alternative strategies for propensity score adjustment producing similarly unsatisfactory covariate balance. The direct adjustment for ZIP code level covariates in the dose-response models is expected to account for residual confounding, but should nonetheless be interpreted with caution due to the reliance on parametric modeling assumptions. Other, more flexible approaches to adjust for confounding deserve further exploration particularly those that might explicitly account for spatial correlation. Concerns about the particular form of confounding adjustment notwithstanding, the analysis presented here adjusted for many features of power plants, population demographics, and weather, but a key source of potential unmeasured confounding is $PM_{2.5}$ that derives from sources *other* than coal-fired power plants, for example, from vehicular traffic. The ignorability assumption in (2) states other types of pollution do not systematically vary with IHD hospitalization rates and the presence of scrubbers on power plants, conditional on the observed covariates. Plausibility of the ignorability assumption relates to the presumption that other sources of $PM_{2.5}$ are likely related to measured ZIP code metrics such as population density. Nonetheless, the threat of unmeasured confounding remains. Finally, the analysis pursued here condenses the clearly time-varying nature of the interventions and network structure to a single annual summary. Scrubbers are installed on additional power plants over time, and the underlying dynamics of pollution transport vary continuously, with particularly pronounced seasonal variation within a year as well as decades-long variation owing to other atmospheric changes. Thus, while we construe T to be fixed at its annual summary, in reality the structure of the network interference evolves over time. Further development of time-varying treatments on time-varying interference networks is an important area of future work that holds particular relevance to the analysis of power plant regulations.

References

Alberto Abadie, Susan Athey, Guido W. Imbens, and Jeffrey M. Wooldridge. Sampling-based vs. Design-based Uncertainty in Regression Analysis. *arXiv:1706.01778 [econ, math, stat]*, June 2019. URL <http://arxiv.org/abs/1706.01778>. arXiv: 1706.01778.

Weihua An. Causal Inference with Networked Treatment Diffusion. *Sociological Methodology*, 48(1):152–181, August 2018. ISSN 0081-1750. doi: 10.1177/0081175018785216. URL <https://doi.org/10.1177/0081175018785216>.

Weihua An and Tyler J. VanderWeele. Opening the Blackbox of Treatment Interference: Tracing Treatment Diffusion through Network Analysis. *Sociological Methods & Research*, page 0049124119852384, August 2019. ISSN 0049-1241. doi: 10.1177/0049124119852384. URL <https://doi.org/10.1177/0049124119852384>.

Peter M. Aronow and Cyrus Samii. Estimating average causal effects under general interference, with application to a social network experiment. *The Annals of Applied Statistics*, 11(4):1912–1947, December 2017. ISSN 1932-6157, 1941-7330. doi: 10.1214/16-AOAS1005. URL <https://projecteuclid.org/euclid.aoas/1514430272>.

Jake Bowers, Mark M. Fredrickson, and Costas Panagopoulos. Reasoning about interference between units: a general framework. *Political Analysis*, 21(1):97–124, 2013. URL <http://pan.oxfordjournals.org/content/21/1/97.short>.

Joan A. Casey, Jason G. Su, Lucas R. F. Henneman, Corwin Zigler, Andreas M. Neophytou, Ralph Catalano, Rahul Gondalia, Yu-Ting Chen, Leanne Kaye, Sarah S. Moyer, Veronica Combs, Grace Simrall, Ted Smith, James Sublett, and Meredith A. Barrett. Improved asthma outcomes observed in the vicinity of coal power plant retirement, retrofit and conversion to natural gas. *Nature Energy*, 5(5):398–408, May 2020. ISSN 2058-7546. doi: 10.1038/s41560-020-0600-2. URL <https://www.nature.com/articles/s41560-020-0600-2>. Number: 5 Publisher: Nature Publishing Group.

Lauraine G. Chestnut and David M. Mills. A fresh look at the benefits and costs of the US acid rain program. *Journal of Environmental Management*, 77(3):252–266, 2005. URL <http://www.sciencedirect.com/science/article/pii/S0301479705002124>.

Francesca Dominici, Michael Greenstone, and Cass Sunstein. Particulate Matter Matters. *Science*, In Press, 2014.

Laura Dwyer-Lindgren, Ali H. Mokdad, Tanja Srebotnjak, Abraham D. Flaxman, Gillian M. Hansen, and Christopher JL Murray. Cigarette smoking prevalence in US counties: 1996-2012. *Population Health Metrics*, 12(1):5, March 2014. ISSN 1478-7954. doi: 10.1186/1478-7954-12-5. URL <https://doi.org/10.1186/1478-7954-12-5>.

Laura Forastiere, Fabrizia Mealli, Albert Wu, and Edoardo Airoldi. Estimating Causal Effects Under Interference Using Bayesian Generalized Propensity Scores. *arXiv:1807.11038 [stat]*, July 2018. URL <http://arxiv.org/abs/1807.11038>. arXiv: 1807.11038.

Laura Forastiere, Edoardo M. Airoldi, and Fabrizia Mealli. Identification and Estimation of Treatment and Interference Effects in Observational Studies on Networks. *Journal of the American Statistical Association*, 0(0):1-18, June 2020. ISSN 0162-1459. doi: 10.1080/01621459.2020.1768100. URL <https://doi.org/10.1080/01621459.2020.1768100>. Publisher: Taylor & Francis eprint: <https://doi.org/10.1080/01621459.2020.1768100>.

Andrew Giffin, Brian Reich, Shu Yang, and Ana Rappold. Generalized propensity score approach to causal inference with spatial interference. *arXiv:2007.00106 [stat]*, June 2020. URL <http://arxiv.org/abs/2007.00106>. arXiv: 2007.00106.

Daniel J. Graham, Emma J. McCoy, and David A. Stephens. Quantifying the effect of area deprivation on child pedestrian casualties by using longitudinal mixed models to adjust for confounding, interference and spatial dependence. *Journal of the Royal Statistical Society: Series A (Statistics in Society)*, 176(4):931-950, 2013. ISSN 1467-985X. doi: 10.1111/j.1467-985X.2012.01071.x. URL <http://onlinelibrary.wiley.com/doi/10.1111/j.1467-985X.2012.01071.x/abstract>.

Lucas R. F. Henneman, Christine Choirat, Cesunica Ivey, Kevin Cummiskey, and Corwin M. Zigler. Characterizing population exposure to coal emissions sources in the United States using the HyADS model. *Atmospheric Environment*, 203:271-280, April 2019a. ISSN 1352-2310. doi: 10.1016/j.atmosenv.2019.01.043. URL <http://www.sciencedirect.com/science/article/pii/S1352231019300731>.

Lucas R. F. Henneman, Christine Choirat, and Corwin M. Zigler. Accountability Assessment of Health Improvements in the United States Associated with Reduced Coal Emissions Between 2005 and 2012. *Epidemiology*, 30(4):477, July 2019b. ISSN 1044-3983. doi: 10.1097/EDE.0000000000001024. URL https://journals.lww.com/epidem/Fulltext/2019/07000/Accountability_Assessment_of_Health_Improvements.3.aspx.

Keisuke Hirano and Guido W. Imbens. The Propensity Score with Continuous Treatments. In *Applied Bayesian Modeling and Causal Inference from Incomplete-Data Perspectives*, pages 73–84. John Wiley & Sons, Ltd, 2004. ISBN 978-0-470-09045-9. doi: 10.1002/0470090456.ch7. URL <https://onlinelibrary.wiley.com/doi/abs/10.1002/0470090456.ch7>.

Michael Hudgens and Elizabeth Halloran. Toward causal inference with interference. *Journal of the American Statistical Association*, 103(482):832–842, June 2008.

G. W. Imbens. The role of the propensity score in estimating dose-response functions. *Biometrika*, 87(3):706–710, September 2000. ISSN 0006-3444. doi: 10.1093/biomet/87.3.706. URL <https://academic.oup.com/biomet/article/87/3/706/293734>.

E. Kalnay, M. Kanamitsu, R. Kistler, W. Collins, D. Deaven, L. Gandin, M. Iredell, S. Saha, G. White, J. Woollen, Y. Zhu, A. Leetmaa, B. Reynolds, M. Chelliah, W. Ebisuzaki, W. Higgins, J. Janowiak, K. C. Mo, C. Ropelewski, J. Wang, Roy Jenne, and Dennis Joseph. The NCEP/NCAR 40-Year Reanalysis Project. *Bulletin of the American Meteorological Society*, 77:437–472, March 1996. doi: 10.1175/1520-0477(1996)077<437:TNYRP>2.0.CO;2. URL <http://adsabs.harvard.edu/abs/1996BAMS...77..437K>.

Vishesh Karwa and Edoardo M. Airoldi. A systematic investigation of classical causal inference strategies under mis-specification due to network interference. *arXiv:1810.08259 [stat]*, October 2018. URL <http://arxiv.org/abs/1810.08259>. arXiv: 1810.08259.

L. Liu, M. G. Hudgens, and S. Becker-Dreps. On inverse probability-weighted estimators in the presence of interference. *Biometrika*, 103(4):829–842, December 2016. ISSN 0006-3444. doi: 10.1093/biomet/asw047. URL <https://academic.oup.com/biomet/article/103/4/829/2659035>.

Lan Liu and Michael G. Hudgens. Large Sample Randomization Inference of Causal Effects in the Presence of Interference. *Journal of the American Statistical Association*, 109(505):288–301, January 2014. ISSN 0162-1459. doi: 10.1080/01621459.2013.844698. URL <http://dx.doi.org/10.1080/01621459.2013.844698>.

Georgia Papadogeorgou, Fabrizia Mealli, and Corwin M. Zigler. Causal inference with interfering units for cluster and population level treatment allocation programs. *Biometrics*, 75(3):778–787, 2019. ISSN 1541-0420. doi: 10.1111/biom.13049. URL <https://onlinelibrary.wiley.com/doi/abs/10.1111/biom.13049>. eprint: <https://onlinelibrary.wiley.com/doi/pdf/10.1111/biom.13049>.

Carolina Perez-Heydrich, Michael G. Hudgens, M. Elizabeth Halloran, John D. Clemens, Mohammad Ali, and Michael E. Emch. Assessing effects of cholera vaccination in the presence of interference. *Biometrics*, May 2014. ISSN 1541-0420. doi: 10.1111/biom.12184.

C. A Pope III, M. Ezzati, and D. W Dockery. Fine-particulate air pollution and life expectancy in the United States. *New England Journal of Medicine*, 360(4):376–386, 2009.

Paul R. Rosenbaum and Donald B. Rubin. The Central Role of the Propensity Score in Observational Studies for Causal Effects. *Biometrika*, 70(1):41–55, April 1983. ISSN 00063444. URL <http://www.jstor.org/stable/2335942>.

Fredrik Sävje, Peter M. Aronow, and Michael G. Hudgens. Average treatment effects in the presence of unknown interference. *arXiv:1711.06399 [math, stat]*, November 2017. URL <http://arxiv.org/abs/1711.06399>. arXiv: 1711.06399.

Elizabeth A. Stuart. Matching methods for causal inference: A review and a look forward. *Statistical science : a review journal of the Institute of Mathematical Statistics*, 25(1):1–21, February 2010. ISSN 0883-4237. doi: 10.1214/09-STS313.

Eric J. Tchetgen Tchetgen and Tyler J. VanderWeele. On causal inference in the presence of interference. *Statistical Methods in Medical Research*, 21(1):55–75, February 2012. ISSN 0962-2802, 1477-0334. doi: 10.1177/0962280210386779. URL <http://smm.sagepub.com/content/21/1/55>.

George D. Thurston, Richard T. Burnett, Michelle C. Turner, Yuanli Shi, Daniel Krewski, Ramona Lall, Kazuhiko Ito, Michael Jerrett, Susan M. Gapstur, W. Ryan Diver, and C. Arden Pope. Ischemic Heart Disease Mortality and Long-Term Exposure to Source-Related Components of U.S. Fine Particle Air Pollution. *Environmental Health Perspectives*, 124(6):785–794, 2016. ISSN 1552-9924. doi: 10.1289/ehp.1509777.

Mark J. Van der Laan. Causal Inference for a Population of Causally Connected Units. *Journal of Causal Inference*, 2(1):13–74, March 2014. ISSN 2193-3677, 2193-3685. doi: 10.1515/jci-2013-0002. URL <https://www.degruyter.com/view/journals/jci/2/1/article-p13.xml>. Publisher: De Gruyter Section: Journal of Causal Inference.

Natalya Verbitsky-Savitz and Stephen W. Raudenbush. Causal inference under interference in spatial settings: a case study evaluating community policing program in Chicago. *Epidemiologic Methods*, 1(1):107–130, 2012. URL <http://www.degruyter.com/view/j/em.2012.1.issue-1/2161-962X.1020/2161-962X.1020.xml>.

Corwin M. Zigler and Georgia Papadogeorgou. Bipartite Causal Inference with Interference.
Statistical Science, To appear, 2020. URL [sjav](#). arXiv: 1807.08660.